2010 11th Int. Conf. Control, Automation, Robotics and Vision
Singapore, 7-10th December 2010

Random Force based Algorithm for Local Minima Escape of Potential Field Method

Jinseok Lee, Yunyoung Nam and Sangjin Hong
Department of Electrical and Computer Engineering
Mobile System Design Laboratory
Stony Brook University - SUNY
Stony Brook, NY, USA
{jinlee, yynam, snjhong}@ece.sunysb.edu

***Abstract*— We address a new inherent limitation of potential field methods, which is symmetrically aligned robot-obstacle-goal (SAROG). The SAROG involves one critical risk of local minima trap. For dealing with the problem, we investigate the way how the local minima trap is recognized, and present our random force algorithm. The force algorithm has two categories of random unit total force (RUTF) and random unit total force with repulsion removal (RUTF-RR) which are selected based on the conditions of a robot, an obstacle and a goal.**

I. Introduction

For autonomous robot navigation, the potential field methods have been widely adopted due to its simplicity and mathematical elegance [1][2]. However, the method has some inherent limitations such as local minima trap. The trap situations occur when a robot runs into a dead end, and a robot never reach a goal [3]. To deal with the issue, tn the previous studies, [4] used harmonic functions with Laplace's equation for eliminating the local minima. The method effectively obviates the local minima problem with the Laplace equation. [5] eliminated the local minima by filling up the entire local minima region. Such new potential functions have been actively proposed [3][6]. Together with the new potential functions, multi-potential functions were also considered [7]. In the method, when a local minima is found in one potential field, another potential map with different resolution ignores the local minima.

In this paper, we address the new limitation of the potential field methods, where a robot, an obstacle and a goal are symmetrically aligned. Such order placement is one of the most challenging issues of local minima trap. None of existing algorithms cannot solve the problem. Recently, the method using virtual obstacle [8][9] has been widely used for local minima escape. However, in the method, the positions and shapes of a robot and an obstacle are non-aligned and/or asymmetric. When the virtual obstacles symmetrically exert the repulsive forces on a robot, and a goal is positioned aligned with the robot and the obstacle, the robot moves back and forth only by endlessly falling into the local minima trap. We refer to the problem of symmetrically aligned robot-obstacle-goal as SAROG. Fig. 1 illustrates the local minima trap problem on SAROG. For simplicity, the problems are depicted by representing a robot, an obstacle and a goal with a point mass in two-dimension coordinates. In case of the local minima trap, a robot moves back and forth between the two positions A and B. In the position A, the attractive force is stronger than the repulsive force. For dealing with the problems of local minima trap on SAROG, we propose new algorithm by using random forces.

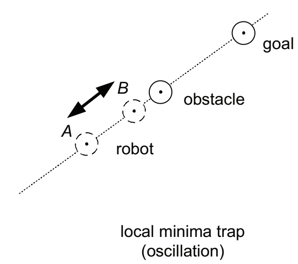

Fig. 1. Illustration of the local minima trap on on SAROG

The remainder of this paper has 5 sections. Section II briefly explains the potential field method and describes problems corresponding to SAROG. In Section III, we propose new algorithm for local minim trap escape. In the algorithm, random unit total force (RUTF) and random unit total force with repulsion removal (RUTF-RR) are presented. Section IV verifies the proposed algorithm using WiRobot X80. Finally, our contribution is summarized in Section V.

II. Potential Field Method and SAROG Problem

A. Potential Field Methods

A robot, an obstacle and a goal are represented by a point mass in two-dimension coordinates. Given a space with size $X_s \times Y_s$, each position is denoted by $\mathbf{p} = [x \quad y]^T$, where $0 \le x \le X_s$ and $0 \le y \le Y_s$. Each position of a robot, an obstacle and a goal are denoted by $\mathbf{p}_r = [x_r \quad y_r]^T$, $\mathbf{p}_o = [x_o \quad y_o]^T$ and $\mathbf{p}_g = [x_g \quad y_g]^T$.

In the potential field method, an attractive potential is defined as a function of the relative distance between a robot and a goal while a repulsive potential is defined as a function of the relative distance between a robot and an obstacle. The two potential functions are commonly expressed as [2][10]

$$U_{att}(\mathbf{p}) = c_{att} \cdot \left(\rho(\mathbf{p}, \mathbf{p}_g)\right)^m , \tag{1}$$

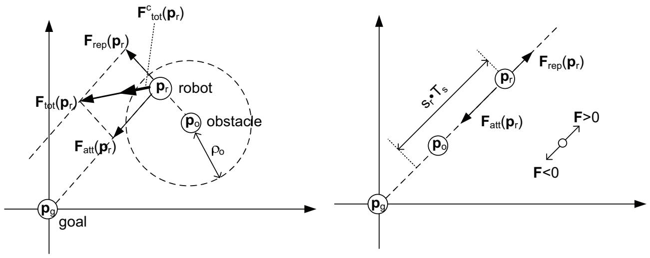

(a) $\mathbf{F}_{tot}(\mathbf{p}_r)$ and $\mathbf{F}^c_{tot}(\mathbf{p}_r)$ (b) Effect of $s_r\dot{T}_s$

Fig. 2. The potential field method and its problem description

$$U_{rep}(\mathbf{p}) = \begin{cases} c_{rep} \cdot \left(\frac{1}{\rho(\mathbf{p},\mathbf{p}_o)} - \frac{1}{\rho_0}\right)^n & \text{if } \rho(\mathbf{p},\mathbf{p}_o) \le \rho_0 \\ 0 & \text{if } \rho(\mathbf{p},\mathbf{p}_o) > \rho_0 \end{cases}, \quad (2)$$

where c_{att} and c_{rep} are constant values for an attractive potential and a repulsive potential. $\rho(\mathbf{p}_1,\mathbf{p}_2)$=$||\mathbf{p}_1,\mathbf{p}_2||$ is the shortest distance between $\mathbf{p}_1$ and $\mathbf{p}_2$. ρ_0 is a positive constant denoting the distance influence of an obstacle.

The corresponding attractive force and repulsive force are then given by the negative gradient of each attractive potential and repulsive potential as

$$\mathbf{F}_{att}(\mathbf{p}) = -m \cdot c_{att} \cdot \left(\rho(\mathbf{p},\mathbf{p}_g)\right)^{m-1} \cdot \nabla\rho(\mathbf{p},\mathbf{p}_g), \quad (3)$$

$$\mathbf{F}_{rep}(\mathbf{p}) = \begin{cases} n \cdot c_{rep} \cdot \left(\frac{1}{\rho(\mathbf{p},\mathbf{p}_o)} - \frac{1}{\rho_0}\right)^{n-1} & \\ \cdot \left(\frac{1}{\rho(\mathbf{p},\mathbf{p}_o)}\right)^2 \cdot \nabla\rho(\mathbf{p},\mathbf{p}_o) & \text{if } \rho(\mathbf{p},\mathbf{p}_o) \le \rho_0 \\ 0 & \text{if } \rho(\mathbf{p},\mathbf{p}_o) > \rho_0 \end{cases}, \quad (4)$$

where $\nabla\rho(\mathbf{p},\mathbf{p}_o)$ and $\nabla\rho(\mathbf{p},\mathbf{p}_g)$ are two unit vectors pointing from $\mathbf{p}_o$ to $\mathbf{p}$ and from $\mathbf{p}_g$ to $\mathbf{p}$, respectively.

The total force applied to each position $\mathbf{p}$ is the sum of the attractive force and the repulsive force as $\mathbf{F}_{tot}(\mathbf{p}) = \mathbf{F}_{att}(\mathbf{p}) + \mathbf{F}_{rep}(\mathbf{p})$, which determines the robot direction and speed for reaching a goal with an obstacle avoidance. As mentioned in the previous section, we consider that a robot moves with constant speed. Thus, the total force $\mathbf{F}_{tot}(\mathbf{p})$ can be re-formulated as $\mathbf{F}^c_{tot}(\mathbf{p}) = \frac{\mathbf{F}_{tot}(\mathbf{p})}{|\mathbf{F}_{tot}(\mathbf{p})|} = \frac{\mathbf{F}_{att}(\mathbf{p})+\mathbf{F}_{rep}(\mathbf{p})}{|\mathbf{F}_{att}(\mathbf{p})+\mathbf{F}_{rep}(\mathbf{p})|}$, where $\mathbf{F}^c_{tot}$ is the total force in the condition of constant robot speed. Then, given the speed $s_r(m/s)$ and sampling time $T_s(s)$, a robot moves $s_r \cdot T_s$ with the direction of $\mathbf{F}^c_{tot}(\mathbf{p})$ or $(\mathbf{F}_{att}(\mathbf{p}) + \mathbf{F}_{rep}(\mathbf{p}))/(|\mathbf{F}_{att}(\mathbf{p}) + \mathbf{F}_{rep}(\mathbf{p})|)$ every T_s. Fig. 2(a) illustrates the forces $\mathbf{F}_{tot}(\mathbf{p}_r)$ and $\mathbf{F}^c_{tot}(\mathbf{p}_r)$ onto a robot by addition of the attractive force $\mathbf{F}_{att}(\mathbf{p}_r)$ and the repulsive force $\mathbf{F}_{rep}(\mathbf{p}_r)$. Throughout this paper, we call $\mathbf{F}^c_{tot}$ a unit total force. Similarly, we call $\mathbf{F}^c_{att}$ and $\mathbf{F}^c_{rep}$ a unit attractive force and a unit repulsive force.

B. *Problem Description*

When $|\mathbf{F}_{att}(\mathbf{p}_r)| < |\mathbf{F}_{rep}(\mathbf{p}_r)|$, a robot moves away from a goal and an obstacle until $|\mathbf{F}_{att}(\mathbf{p}_r)| > |\mathbf{F}_{rep}(\mathbf{p}_r)|$. Then the robot moves back toward an obstacle and a goal, and finally oscillates between two positions. The local minima problem condition is summarized as

$$\begin{aligned} |\mathbf{F}_{att}(\mathbf{p}_r)| &> |\mathbf{F}_{rep}(\mathbf{p}_r)|, & (5)\\ \rho(\mathbf{p}_r,\mathbf{p}_o) &> s_r \cdot T_s, & (6)\\ \nabla\rho(\mathbf{p}_r,\mathbf{p}_o) &= \nabla\rho(\mathbf{p}_r,\mathbf{p}_g). & (7) \end{aligned}$$

The local minima problem on the condition of constant robot speed and SAROG have not been addressed yet, and it should be taken into account to deal with the local minima trap (oscillation). However, a question arises: when a robot is not initially aligned with an obstacle and a goal, the condition of SAROG is negligible. However, the SAROG occurs even when a robot, an obstacle and a goal are not initially aligned. As illustrated in Fig. 3, consider that a robot is initially positioned at (1.0m,1.0m), an obstacle is positioned at (5.0m,5.0m), and a goal is positioned at (5.4m,4.6m). A robot speed s_r is $\sqrt{2}m/s$, and sampling time T_s is 1 second. In addition, we set up m=2, n=2, ρ=1, c_{att}=0.5 and c_{rep}=5. Throughout this paper, unless otherwise noted, s_r, T_s, m, n, ρ, c_{att} and c_{rep} are as above.

As shown in Fig. 3(a), at the sampling time 0, a robot, an obstacle and a goal are not initially aligned. However, when a robot moves closer to a goal, a robot finally oscillates between two points A and B by not reaching a goal as illustrated in Fig. 3(b). Thus, the SAROG may occur when an obstacle and a goal closely positioned even though the initial positions of a robot, an obstacle and a goal are not aligned.

III. Local Minima Escape Algorithm

A. *Random Force Algorithm for Local Minima Escape*

1) Recognition of Local Minima Trap: On the conditions of constant speed and SAROG, the local minima problem is categorized into two cases. Fig. 4 illustrates the two cases of local minima trap. One case is that a robot is trapped in local minima before arriving a goal (i.e. oscillating across non-goal area). The other case is that a robot is trapped after arriving a goal (i.e. oscillating across a goal). Thus, in order to deal with the the local minima trap, a robot should first recognize whether it is trapped across a goal or non-goal area. As illustrated in Fig. 4(a) when a robot is trapped across a non-goal area, the attractive forces of positions A and B are formed with same direction, but the total forces of the two positions are formed with opposite direction. On the other hand, as illustrated in Fig. 4(b) when a robot is trapped across a goal, both the attractive forces and the total forces of positions A and B are formed with opposite direction. Thus, a robot is trapped across a non-goal when the conditions are formed

$$\mathbf{F}^c_{tot}(\mathbf{A}) = -\mathbf{F}^c_{tot}(\mathbf{B}) \text{ and } \mathbf{F}^c_{att}(\mathbf{A}) = \mathbf{F}^c_{att}(\mathbf{B}), \quad (8)$$

and a robot is trapped across a goal when conditions are formed

$$\mathbf{F}^c_{tot}(\mathbf{A}) = -\mathbf{F}^c_{tot}(\mathbf{B}) \text{ and } \mathbf{F}^c_{att}(\mathbf{A}) = -\mathbf{F}^c_{att}(\mathbf{B}). \quad (9)$$

On the local minima condition of (9), a robot should find the path to reach the exact goal. For a solution, [11] proposed new potential functions for the problem named goals nonreachable with obstacles nearby (GNRON).

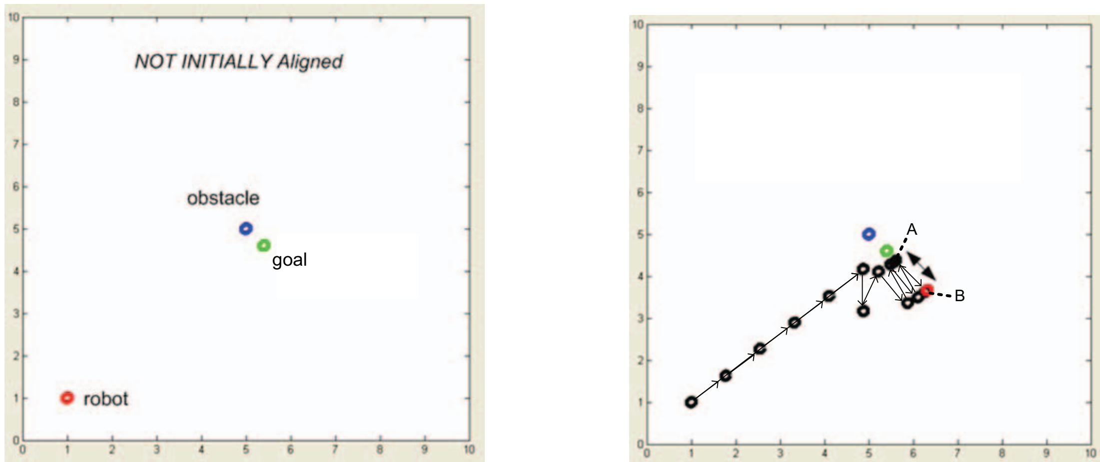

(a) At time-instant 0

(b) From time-instant 13

Fig. 3. The SAROG based local minima occurs even when a robot, an obstacle and a goal are not initially aligned

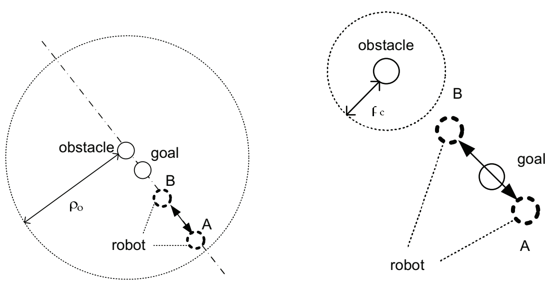

(a) A robot trapped before arriving a goal.

(b) A robot trapped after arriving a goal.

Fig. 4. Two cases of local minima trap on SAROG and constant robot speed

2) Random Force Algorithm for Local Minima Across Non-Goal: On the condition of (8), a robot should find the path to escape the local minima. For the path, we use a random unit total force (RUTF). The RUTF determines the robot direction and the robot escapes the local minima. After the RUTF exertion, the original potential force is continuously used until the condition of (8) arises. Thus, the random force algorithm alternates potential based motions with the random motion.

Fig. 5 shows the effect of the RUTF based algorithm. A robot starts to move from (1.0m, 1.0m) with an obstacle positioned at (3.0m, 3.0m) and a goal positioned at (4.0m, 4.0m). The robot moves toward the goal of point (4.0m, 4.0m) with $s_r = 0.4m/s$ and $T_s = 1s$. When the forces to exerting the robot are satisfied with (8), a robot recognizes the local minima across non-goal. Then, we exert a random unit total force (RUTF) onto a robot as shown in Fig. 5(a). The RUTF helps a robot escape from the oscillation. After escaping from the oscillation, the robot continuously moves toward the goal (4.0m, 4.0m) by potential based forces as shown in Fig. 5(b).

However, the RUTF based local minima escape is not applicable when a robot is positioned closer to a goal than an obstacle: the placement order is robot-goal-obstacle. To illustrate the case, consider that a robot is positioned at (1.0m,1.0m), an obstacle is positioned at (3.4m,3.4m) and a goal is positioned at (3.0m,3.0m) as shown in Fig. 6(a). From the time-instants 0 to 6, a robot moves close to a goal. At time-instant 6, the local minima across non-goal is satisfied with (8), and the RUTF exerts onto a robot resulting in the movement as shown in Fig. 6(a). After the robot escapes from the local minima, the robot continuously moves by potential based forces as shown in Fig. 6(b) through Fig. 6(d), where the robot moves back to the local minima. That is, the RUTF based local minima escape is applicable only when $\rho(\mathbf{p}_r, \mathbf{p}_g) > \rho(\mathbf{p}_r, \mathbf{p}_o)$. Otherwise, a robot moves back to previous local minima as shown in Fig. 6(d).

Thus, in the case of $\rho(\mathbf{p}_r, \mathbf{p}_g) < \rho(\mathbf{p}_r, \mathbf{p}_o)$, we use a potential function with repulsion removal as

$$\mathbf{F}^c_{tot}(\mathbf{p}) = \frac{\mathbf{F}^c_{att}(\mathbf{p})}{|\mathbf{F}^c_{att}(\mathbf{p})|}. \tag{10}$$

That is, once the potential forces and the distance conditions are both satisfied with (8) and $\rho(\mathbf{p}_r, \mathbf{p}_g) < \rho(\mathbf{p}_r, \mathbf{p}_o)$, the RUTF changes robot direction and the potential force of (10) exerts onto a robot. The RUTF and the potential function with removal (RUTF-RR) algorithm derives a robot to reach a goal by removing a repulsion force since the movement back to previous local minima after RUTF is from the repulsive force existence. The attractive force exertion of (10) continues until a robot arrives at a goal. When the RUTF-RR is used, the robot collision issue should be considered as well. Since the robot moves with only attractive force, it is possible for the robot to collide with an obstacle. The collision occurs more frequently when the size of a robot and/or an obstacle increases, and the distance between a goal and an obstacle becomes shorter. In order to investigate the anti-collision condition, Fig. 7(a)

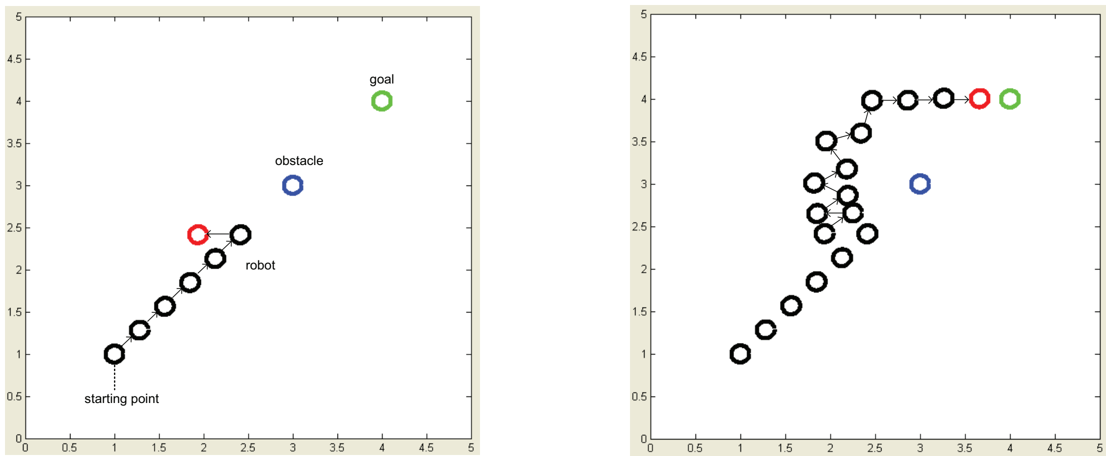

(a) RUTF exertion

(b) After RUTF

Fig. 5. Local minima escape using RUTF

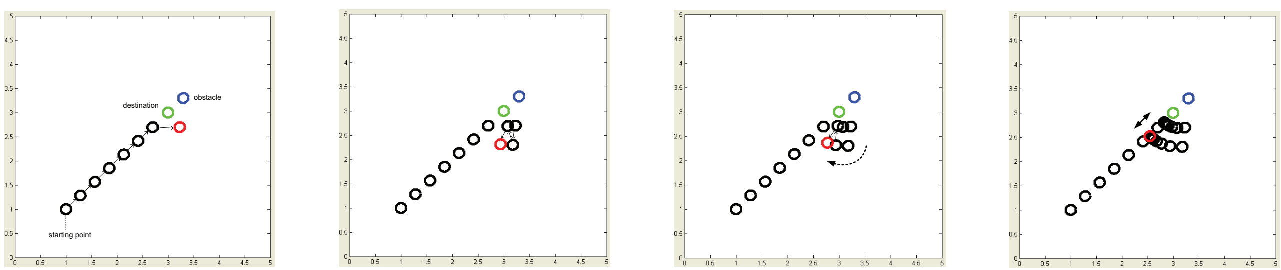

(a) time-instant 0 to 7

(b) time-instant 0 to 10

(c) time-instant 0 to 12

(d) time-instant 0 to 20

Fig. 6. RUTF algorithm limitation: Even though the RUTF exerts onto a robot, the robot eventually moves back to the local minima of SAROG.

illustrates the placement and the size of a robot, a goal and an obstacle. Given the robot position $\mathbf{P}_r$, the RUTF should be generated in the collision free area. Then, after the RUTF exertion to the collision free area, the collision is prevented even with the attraction force only. Fig. 7(a) is re-illustrated in Fig. 7(b) to find the anti-collision condition. The angles θ_1 and θ_2 are formulated as $\theta_1 = \theta_2 = \csc\left(\frac{r_r+r_o}{d_v}\right)$ Then, the shortest distance d_w between a robot and the shaded region boundary is expressed as $d_w = d_u \cdot \sin\theta_1$. In addition, the RUTF angle $\theta(\mathbf{F}^c_{tot})$ is

$$\theta(\mathbf{F}^c_{tot}) = \pi - \theta_1. \tag{11}$$

In order to move inside the shaded region with speed s_r, the robot should keep moving with the force direction $\pm(\pi - \theta_1)$ for τ time-instants, where $\tau = \left\lceil \frac{d_w}{s_r} \right\rceil$. The sign $\pm$ of the force direction is randomly assigned. After τ time-instants, a robot keeps moving by the attraction only.

IV. Algorithm Verification and Analysis

A. Simulation Setup

For the algorithm verification, we used the WiRobot X80 as shown in Fig. 8. The X80 underlies technology evolved from Dr Robot Distributed Computation Robotic Architecture, originally developed for Dr Robot Humanoid Robot. It is developed for fast and strong motion, while itself remaining lightweight and nimble. The wheel-based platform is with two 12V DC motors each supply 22kg·cm of torque to the 18 cm wheels, yielding a top speed in excess of 1 m/s. Two high-resolution with 1200 count per wheel cycle quadrature encoders mounted on each wheel provide high-precision measurement and control of wheel movement. For estimating the distance between a robot and an obstacle, we equipped the robot with three ultrasonic range sensor modules of DUR5200. The range sensor detects an obstacle within 3.4 meters. The distance data is precisely presented by the time interval between the time-instant when the measurement is enabled and the time-instant when the echo signal is received. By using the ultrasonic range sensor modules, the robot recognizes its near obstacle position up to 3.4 meters. For the proposed algorithm verification on the restricted two conditions of SAROG and robot constant speed. we set up the robot, obstacles and the goal as in Fig. 9. Initially, *goal 1* is enabled while *goal 2* and *goal 3* are disabled. After the robot reaches *goal 1*, *goal 2* only is enabled. Finally, after the robot reaches *goal 2*, *goal 3* only is enabled.

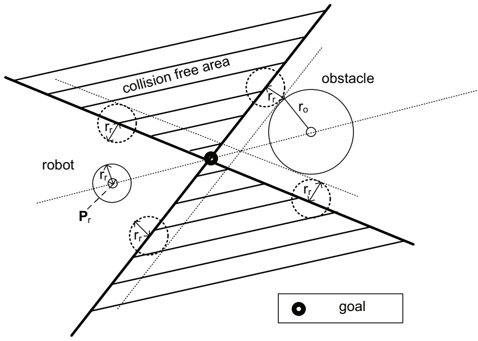

(a) The placement and the size of a robot, a goal and an obstacle

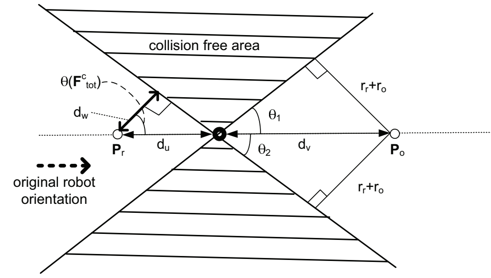

(b) Geometry for d_w and $\theta(\mathbf{F}^c_{tot})$

Fig. 7. Illustration of the anti-collision condition

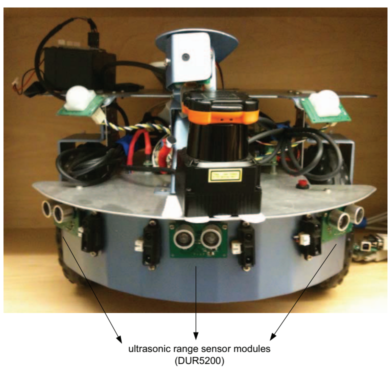

Fig. 8. WiRobot X80: three ultrasonic range sensor modules of DUR5200 are attached for distance estimation.

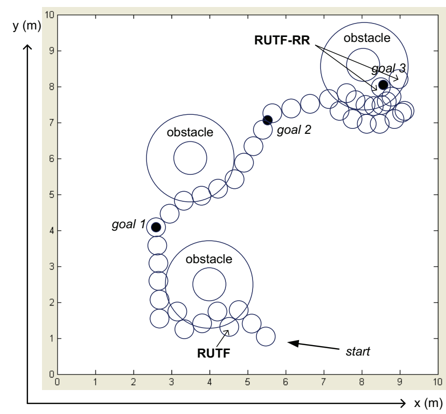

Fig. 9. WiRobot X80 traveled from *Start* to *goal 1*, *goal 2* and *goal 3* in order with RUTF and RUTF-RR algorithms.

For the navigation to *goal 1*, the robot has the problem on SAROG; and thus, will be trapped on local minim by using potential field method only. In the local minima trap, we will show the RUTF will solve the problem. For the navigation to *goal 3*, the robot also has the problem on SAROG; and thus will be trapped on local minima again. However, in the case, the RUTF cannot solve the problem; the robot moves back to original local minima after RUTF. In the local minima trap, we will show the RUTF-RR deals with the problem.

B. Results and Discussion

As depicted in Fig. 9, X80 traveled from *Start* to three goals; *goal 1* positioned at (2.5m,4.0m), *goal 2* positioned at (5.5m,7.0m) and *goal 3* positioned at (8.5m,8.0m). Each obstacle is positioned at (4.0m,2.5m), (3.5m,6.0m) and (8.0m,8.5m) with $r_o = 0.4375m$ and $\rho_o = 1.2m$. The robot starts from the position (5.5m,1.0m) with $r_r = 0.25m$, $T_s = 1s$ and $s_r = 0.5m/s$. With *goal 1* only enabled, the robot first moved toward *goal 1* with potential functions and kept moving until the condition of (8) is satisfied at time 2 (s). At time 2 (s), the robot compared the distance condition, which was $\rho(\mathbf{p}_r, \mathbf{p}_g) > \rho(\mathbf{p}_r, \mathbf{p}_o)$, and RUTF instead of the potential functions determined robot direction for the local minima escape. From 3 (s) to 13 (s), the robot moved toward *goal 1* by using the potential field, and finally arrived at *goal 1*. Once the robot arrived at *goal 1*, *goal 1* was disabled and only *goal 2* was enabled. We set the starting time from *goal 1* to zero. From *goal 1* to *goal 2*, any local minima problem did not occur. Note until time 2 (s), the robot has the potential function involved with attraction force only. From time 2 (s) to 6 (s), the potential function involved both the attraction force and the repulsion force since the robot positioned within the obstacle influence. From 6 (s) to 9 (s), the potential function involved with attraction force only and the robot finally arrived at *goal 2*. Similarly, once the robot arrived at *goal 2*, *goal 2* was disabled and only *goal 3* was enabled. We also set the starting time from *goal 2* to zero. From *goal 2* the robot moved toward *goal 3* with potential functions and kept moving until the condition of (8) is satisfied at time 15 (s). At time 15 (s), the robot compared the distance condition, which was $\rho(\mathbf{p}_r, \mathbf{p}_g) < \rho(\mathbf{p}_r, \mathbf{p}_o)$, and RUTF-RR instead of the potential functions determined robot direction for the local minima escape, and finally let the robot arrived at *goal 3* with $\tau = 1$.

V. Conclusion

We have described new problem of symmetrically aligned robot-obstacle-goal (SAROG) with using potential field methods. For dealing with the corresponding the critical issue of local minima trap, random force based algorithms have been proposed and they have been verified using WiRobot X80 with three ultrasonic range sensor modules.

References

[1] P. Veelaert and W. Bogaerts, "Ultrasonic Potential Field Sensor for Obstacle Avoidance", in *IEEE Transactions on Robotics and Automation*, vol. 15, pp. 774-779, Aug. 1999.

[2] J. Latombe, *Robot Motion Planning.*, Norwell, MA: Kluwer, 1991.

[3] R. Tilove, "Local Obstacle Avoidance for Mobile Robots Based on the Method of Artificial Potentials", in *Proceedings of the IEEE Conference on Robotics and Automation*, Cincinnati, Ohio, May, 1990, pp.566-571.

[4] C. Connolly, J. Burns, R. Weiss, "Path Planning using Lapace's Equation", in *Proceedings of the IEEE International Conference on Robotics and Automation*, pp. 2102-2106, 1990.

[5] E. Rimon, D. Koditscheck, "Exact Robot Navigation using Artificial Potential Functions", in *IEEE Transactions on Robotics and Automation*, vol. 8, No. 5, pp. 501-518, 1992.

[6] J. Ren, K. A. McIsaac and R. V. Patel, "Modified Newton's Method Applied to Potential Field-Based Navigation for Mobile Robots", in *IEEE Transactions on Robotics*, vol. 22, No. 2, pp. 384-390, 2006.

[7] H. Chang, "A New Technique to Handle Local Minimum for Imperfect Potential Field based Motion Planning", in *Proceedings of the IEEE International Conference on Robotics and Automation*, pp. 108-112, 1996.

[8] C. Ordonez, E. G. Collins, M. F. Selekwa and D.D. Dunlap, "The Virtual Wall Approach to Limit Cycle Avoidance for Unmanned Ground Vehicles", in *Elsevier, Robotics and Autonomous Systems*, vol. 56, pp. 645-657, 2008.

[9] V.O.S. Olunloyo and M.K.O. Ayomoh, "Autonomous Mobile Robot Navigation Using Hybrid Virtual Force Field Concept", in *European Journal of Scientific Research*, vol. 31, No. 2, pp. 204-228, 2009.

[10] Y. Koren and J. Borenstein , "Potential Field Methods and Their Inherent Limitations for Mobile Robot Navigation", in *Proceedings of the IEEE Confernce on Robotics and Automation, Sacramento, California*, April, 1991, pp.1398-1404.

[11] S. Ge and Y. Cui, "New Potential Functions for Mobile Robot Path Planning", in *IEEE Transactions on Robotics and Automation*, vol. 16, No. 5, pp. 615-620, Oct. 2000.